The HNF-1 target Collectrin controls insulin exocytosis by SNARE complex formation

Kenji Fukui,[1,9] Qin Yang,[1,9,10] Yang Cao,[1] Noriko Takahashi,[2,3] Hiroyasu Hatakeyama,[2] Haiyan Wang,[4] Jun Wada,[5] Yanling Zhang,[5] Lorella Marselli,[6] Takao Nammo,[1] Kazue Yoneda,[1] Mineki Onishi,[1] Shigeki Higashiyama,[3,7] Yuji Matsuzawa,[1] Frank J. Gonzalez,[8] Gordon C. Weir,[6] Haruo Kasai,[2] Iichiro Shimomura,[1] Jun-ichiro Miyagawa,[1] Claes B. Wollheim,[4] and Kazuya Yamagata[1,*]

[1] Department of Metabolic Medicine, Graduate School of Medicine, Osaka University, Suita Osaka 565-0871, Japan
[2] Department of Cell Physiology, National Institute for Physiological Sciences, and Graduate University of Advanced Studies, Myodaiji, Okazaki 444-8787, Japan
[3] Precursory Research for Embryonic Science and Technology, Japan Science and Technology Agency, 4-1-8, Honcho, Kawaguchi 332-0012, Saitama, Japan
[4] Department of Cell Physiology and Metabolism, University Medical Center, CH-1211 Geneva 4, Switzerland
[5] Department of Medicine and Clinical Science, Graduate School of Medicine and Dentistry, Okayama University, Okayama 700-8558, Japan
[6] Joslin Diabetes Center, One Joslin Place, Boston, Massachusetts 02215
[7] Division of Biochemistry and Molecular Genetics, Department of Cellular and Molecular Biology, Ehime University School of Medicine, Ehime 791-0295, Japan
[8] Laboratory of Metabolism, Center for Cancer Research, National Cancer Institute, and National Institutes of Health, Bethesda, Maryland 20892
[9] These authors contributed equally to this work.
[10] Present address: Division of Endocrinology, Diabetes, and Metabolism, Beth Israel Deaconess Medical Center, Harvard Medical School, Boston, Massachusetts 02215
*Correspondence: kazu@imed2.med.osaka-u.ac.jp

Summary

Defective glucose-stimulated insulin secretion is the main cause of hyperglycemia in type 2 diabetes mellitus. Mutations in HNF-1α cause a monogenic form of type 2 diabetes, maturity-onset diabetes of the young (MODY), characterized by impaired insulin secretion. Here we report that collectrin, a recently cloned kidney-specific gene of unknown function, is a target of HNF-1α in pancreatic β cells. Expression of collectrin was decreased in the islets of HNF-1α (−/−) mice, but was increased in obese hyperglycemic mice. Overexpression of collectrin in rat insulinoma INS-1 cells or in the β cells of transgenic mice enhanced glucose-stimulated insulin exocytosis, without affecting Ca^{2+} influx. Conversely, suppression of collectrin attenuated insulin secretion. Collectrin bound to SNARE complexes by interacting with snapin, a SNAP-25 binding protein, and facilitated SNARE complex formation. Therefore, collectrin is a regulator of SNARE complex function, which thereby controls insulin exocytosis.

Introduction

Insulin is stored in secretory granules in pancreatic β cells and is secreted by exocytosis (Reviewed in Orci, 1974; Lang, 1999, Rorsman and Renström, 2003). The latter process is precisely controlled to achieve blood glucose homeostasis. Defective glucose-stimulated insulin secretion is the main cause of hyperglycemia in type 2 diabetes mellitus (Reviewed in Wollheim, 2000). Maturity-onset diabetes of the young (MODY) is a clinically heterogenous group of disorders accounting for 2%–5% of type 2 diabetes. MODY is characterized by nonketotic diabetes mellitus, an autosomal dominant mode of inheritance, an onset usually before 25 years of age (frequently during childhood or adolescence), and a primary defect of pancreatic β cell function (Reviewed in Fajans et al., 2001). MODY can result from mutations in any of at least six different genes that encode the glycolytic enzyme glucokinase (MODY2) (Froguel et al., 1993) and five transcription factors: hepatocyte nuclear factor (HNF)-4α (MODY1) (Yamagata et al., 1996a), HNF-1α (MODY3) (Yamagata et al., 1996b), insulin promoter factor-1 (IPF-1) (Stoffers et al., 1997), HNF-1β (Horikawa et al., 1997), and neurogenic differentiation 1 (NeuroD1) (Malecki et al., 1999). Two of these MODY genes, HNF-1α and HNF-1β, belong to a subclass of the homeodomain family and they share a highly conserved DNA binding domain composed of an atypical POU-specific, a POU homeodomain and a more divergent C-terminal transactivation domain. In most populations, mutations in the HNF-1α gene are the most common cause of MODY (Reviewed in Fajans et al., 2001). Mutations in the HNF-1β gene are relatively uncommon, causing renal dysfunction as well as diabetes mellitus (Horikawa et al., 1997; Bellanne-Chantelot et al., 2004). Earlier studies indicated that HNF-1α plays an important role in the multifactorial process of insulin secretion including glucose transport, glycolysis and mitochondrial oxidation (Pontoglio et al., 1998; Dukes et al., 1998; Yamagata et al., 2002; Wang et al., 1998, 2000; Yang et al., 2002). However, the molecular mechanisms of MODY3/MODY5 are not fully understood. The purpose of this study was to identify novel molecule(s) involved in the regulation of insulin secretion from β cells by screening the downstream target genes of the HNF-1 transcription factor. Here we report the discovery of collectrin, a recently cloned kidney-specific gene of unknown function, as a novel target of HNF-1α in pancreatic β cells and its implication in insulin exocytosis.

Results

Collectrin is a novel target of HNF-1

P291fsinsC (insertion of a C at codon 291in a polyC tract) is the most common naturally-occurring mutation in the HNF-1α gene, and this frameshift mutant acts in a dominant-negative manner (Yamagata et al., 1998). We previously established a rat-derived β cell line (INS-1) that can overexpress P291fsinsC-HNF-1α under tight control of doxycycline (HNF1α-P291fsinsC#32 cells) (Wang et al., 2000). To identify genes that are specifically down-regulated by the induction of P291fsinsC-HNF-1α, we applied the suppression subtraction hybridization technique with mRNA extracted from doxycycline-induced or noninduced HNF1α-P291fsinsC#32 cells. In the initial step, 376 clones from the subtraction library were selected for analysis. Subsequent differential screening and Northern blotting analysis identified 4 unique genes that were down-regulated by induction of the dominant negative mutant. DNA sequencing revealed that these 4 clones encode collectrin/ Tmem27 (Gene bank No. NM_020976) (Figure 1A), 3-methylcholanthrene-inducible UDP-glucuronosyltransferase (J05132), phosphatidylcholine transfer protein-like (PCTP-L) (NM_019990), and proliferation-associated 2G4 (Pa2g4) (NM_011119). Collectrin was originally reported as a kidney specific gene, displaying increased expression in hypertrophic renal disease (Zhang et al., 2001). Collectrin is a putative glycoprotein that shares homology with the C-terminal of angiotensin-converting enzyme-related carboxypeptidase (ACE2), but lacks the dipeptidyl carboxypeptidase catalytic domains and its biological function is completely unknown (Zhang et al., 2001).

To investigate the transcriptional regulation of the collectrin by HNF-1, we cloned ~500-bp of the 5′ flanking promoter region of the rat collectrin gene. DNA sequencing revealed a high affinity HNF-1 binding site (Tronche et al.,1997) (nucleotides −137 to −122, relative to the translation start codon where the A is numbered with +1) (Figure 1B). Screening of the genomic databank revealed that this binding site was also conserved in the human and mouse collectrin genes. The position of the transcriptional start site was determined to be downstream of the binding site by primer extension analysis (data not shown). Specific binding of HNF-1α and HNF-1β to the putative HNF-1 binding site was demonstrated by electrophoretic mobility shift assay (EMSA) (Figure 1C). The promoter region of collectrin was cloned into pGL3-luciferase vector and cotransfected into INS-1 cells with wild-type (WT)-HNF-1α, WT-HNF-1β or P291fsinsC-HNF-1α expression vectors. WT-HNF-1α and HNF-1β dose-dependently increased collectrin promoter activity, while the dominant negative mutant P291fsinsC-HNF-1α suppressed it (Figure 1D). Disruption of the HNF-1 binding site was associated with an 80% reduction of promoter activity (Figure 1E).

To investigate the influence of HNF-1α on collectrin gene expression in vivo, we measured collectrin mRNA in the islets of HNF-1α mutant mice by real-time quantitative PCR. HNF-1α knockout mice (Lee et al., 1998) and RIP-P291fsinsC-HNF-1α transgenic mice (Yamagata et al., 2002) are two MODY3 mouse models that feature impaired insulin secretion. Collectrin mRNA was detected in pancreatic islets (see below), and its expression was significantly reduced in the islets of RIP-P291fsinsC-HNF-1α transgenic mice compared with their controls (Figure 1F). Collectrin mRNA was also significantly repressed in the islets of HNF-1α knockout mice (0.6% of WT, $p < 0.01$) (Figure 1F). Therefore, both the in vitro and in vivo data indicate that collectrin is a direct target gene of HNF-1α.

Collectrin is expressed in pancreatic β cells

Northern blotting analysis of mouse tissues confirmed a high level of collectrin mRNA expression in the kidney (Figure 2A). We found that collectrin mRNA was also expressed in mouse pancreatic islets, as well as rat INS-1 and mouse MIN6 insulinoma cells (Figure 2A). Although collectrin mRNA was not detected in the human pancreas by a previous study (Zhang et al., 2001), it might be expressed in human islets as is the case in the mouse. To resolve this questions, human pancreatic β cell rich tissue was microdissected by laser capture microdissection from pancreases of four cadaver donors. After RNA extraction and cRNA synthesis, samples were run on Affymetrix microarrays (GeneChip Human X3P Array); the results confirmed the abundant expression of collectrin in human islets. For all of the samples, the probes for collectrin had a present detection call as evaluated by the GeneChip Operating Software (GCOS). The signal strength of collectrin for the four samples was 535, 1535, 1116, and 1146, as determined with dChip software. The median signal strength for the 58,876 genes on the X3P Arrays was 42. To examine collectrin expression at the protein level, we generated an antibody against collectrin protein. The specficity of the antibody was confirmed by a peptide competition study (Figure S1 in the Supplemental Data available with this article online). Western blots of mouse tissue extracts showed that collectrin was expressed in pancreatic islets as well as β cell lines (Figure 2B). In agreement with the results of real-time quantitative PCR (Figure 1F), expression of collectrin protein was not detected in the islets of HNF-1α knockout mice (Figure 2B). The protein expressed in islets (43 kDa), β cell lines (40 kDa) and kidney (38 kDa) was larger than predicted from its sequence (26 kDa). Collectrin contains two N-linked glycosylation sites and one O-glycosylation site. Treatment with N-glycosidase F and O-glycosidase led to a shift in the mobility of collectrin to the expected size (Figure 2C), suggesting that the size difference was due to glycosylation. Immunohistochemical analysis of pancreatic specimens revealed that collectrin was expressed by insulin-positive β cells in both mice and humans (Figure 2D). Collectrin was also present in pancreatic α cells (data not shown), but was not detected in exocrine cells (Figure 2D).

To investigate the potential role of collectrin in β cells, we measured its levels in mouse islets under physiological and pathological conditions. Figure 2E shows the effect of fasting and re-feeding on collectrin mRNA expression in the islets. Collectrin mRNA was significantly increased in the islets by re-feeding, suggesting its physiological regulation. Next, we measured collectrin in two obese animal models, i.e., high-fat diet obese C57Bl/6 (HF) mice and KKAy mice. Both HF mice (fed for 15 weeks) and KKAy mice (13-week-old) were obese and showed hyperglycemia compared with their controls (Body weight: HF 44.1 ± 1.7 g, control 29.1 ± 1.7 g, KKAy 47.9 ± 1.2 g, control 23.1 ± 0.6 g. Blood glucose levels: HF 179.6 ± 3.8 mg/dl, control 141.8 ± 7.5 mg/dl, KKAy 272.2 ± 38.7 mg/dl, control 120.0 ± 6.7 mg/dl). In the two mouse models, insulin secretion is increased to compensate for insulin resistance (Winzell and Ahren, 2004; Nishizawa et al., 2004). Plasma insulin levels were significantly increased in the obese HF mice (9.8 ± 0.9 ng/ml) compared with lean control mice (1.9 ± 0.6 ng/ml) and collectrin mRNA levels were elevated

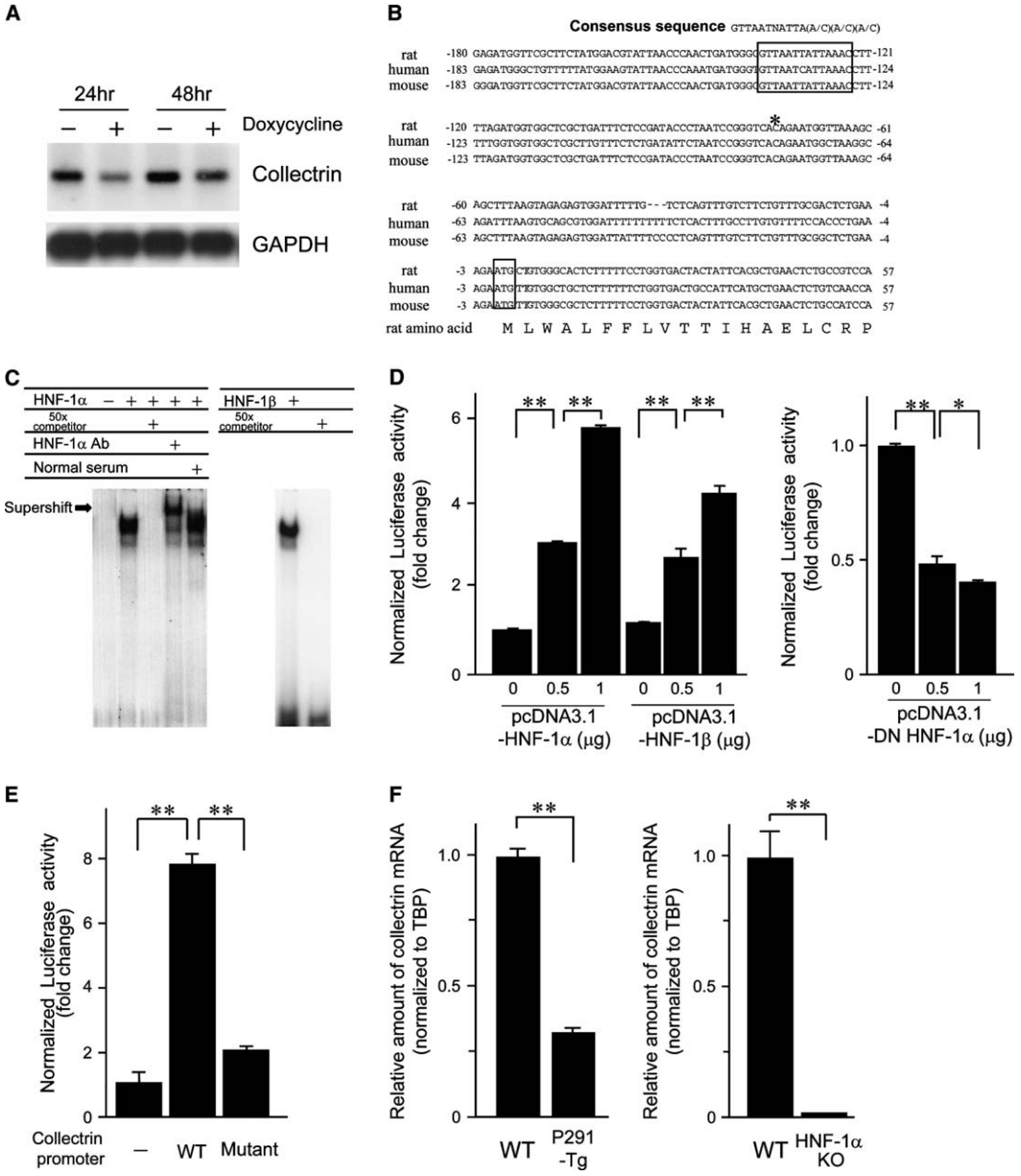

Figure 1. Transcriptional regulation of the collectrin gene by HNF-1

A) Effect of P291fsinsC-HNF-1α on collectrin mRNA tested by Northern blotting. Total RNA was obtained from uninduced or induced (500 ng/ml doxycycline) HNF1α-P291fsinsC#32 cells.

B) DNA sequences of the rat, mouse, and human promoter and 5′-flanking regions. The putative HNF-1 binding site is shown by a box. The asterisk denotes the transcription start site.

C) EMSA analysis of the HNF-1 binding site in the collectrin gene promoter. DNA binding was tested using nuclear extracts of HeLa cells, which were transfected with pcDNA3.1-HNF-1α or pcDNA3.1-HNF-1β.

D and E) The collectrin gene promoter is activated by HNF-1. INS-1 cells were cotransfected with the indicated amounts of the expression vectors as well as 0.5 μg of pGL3-collectrin reporter and 10 ng of pRL-TK vector. (**D**) INS-1 cells were transfected with 0.5 μg of pcDNA3.1-HNF-1α as well as 0.5 μg of pGL3-collectrin reporter (WT or mutant) and 10 ng of pRL-TK vector (**E**). Data are mean ± SEM from three independent experiments. *$p < 0.05$, **$p < 0.01$.

F) Expression of collectrin mRNA in pancreatic islets of MODY3 model mice. Total RNA was extracted from the islets of P291fsinsC-HNF-1α transgenic mice (P291-Tg), HNF-1α KO (−/−) mice and their control littermates for real-time RT-PCR. Data are the mean ± SEM from three independent experiments. **$p < 0.01$.

by 2.0-fold in the islets of HF mice (Figure 2F). Furthermore, the protein levels were also increased 2.6-fold in the HF mice. Expression of collectrin was also significantly elevated in KKAy mice (1.6-fold) compared with their lean controls (Figure 2G). Thus collectrin expression was decreased in MODY3 model mice parallel to impaired insulin secretion and was increased in the obese mice. This suggests that collectrin may play a role in insulin secretion.

Collectrin enhances insulin secretion in vitro

We generated stable transformants by transfecting an expression vector coding myc-tagged human collectrin cDNA

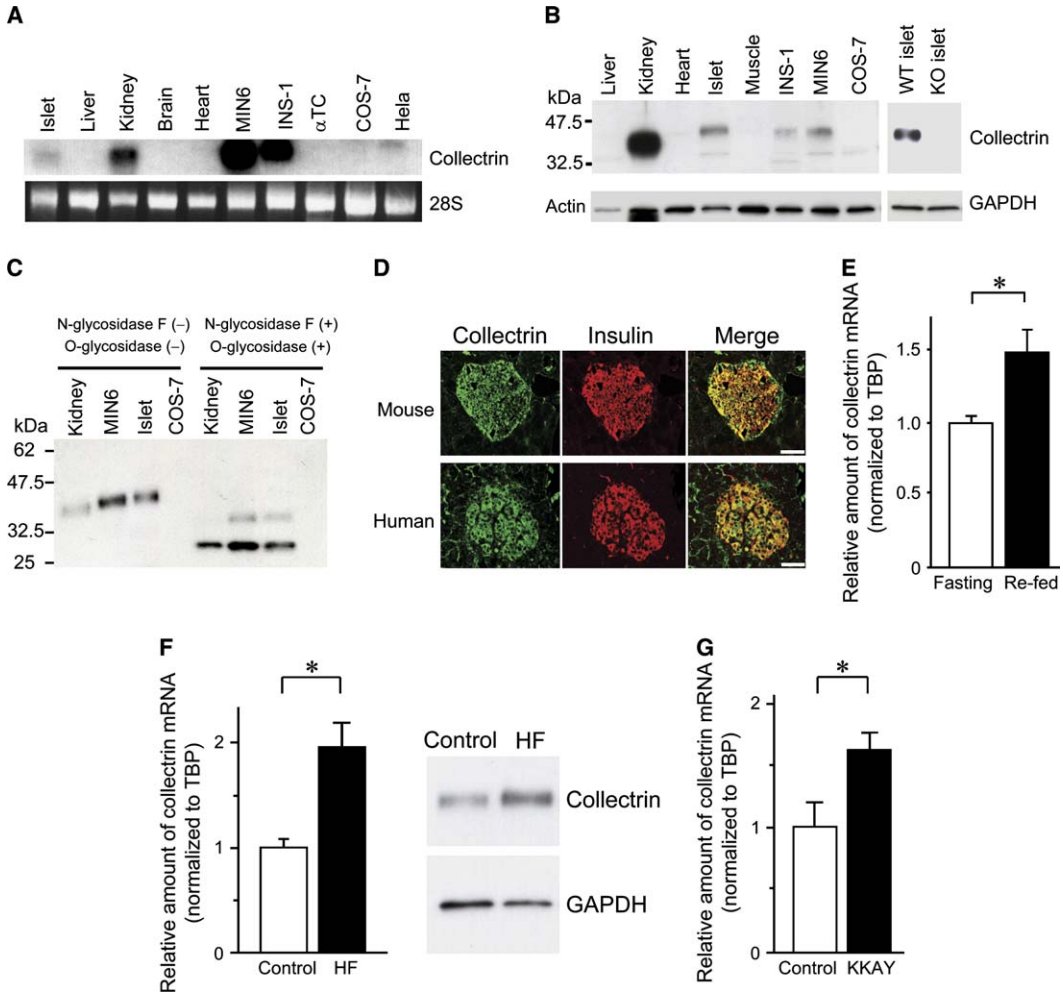

Figure 2. In vivo expression of collectrin mRNA under physiological and pathological conditions

A) Northern blotting analysis of collectrin gene expression. Collectrin mRNA was expressed in both pancreatic islets and β cell lines.

B) Western blotting analysis of collectrin. Collectrin was expressed in mouse pancreatic islets and β cell lines, as well as in kidney. Expression of collectrin was not detected in the islets of HNF-1α KO mice.

C) N-glycosidase F and O-glycosidase treatment of collectrin. 0.5 μg of protein (kidney) and 4 μg of protein (MIN6, COS-7 cells and islets) were treated with N-glycosidase F and O-glycosidase and subjected to Western blotting with anti-collectrin antibody.

D) Expression of collectrin in pancreatic β cells. Sections of C57BL6 mouse pancreas and human pancreas were immunostained with anti-collectrin antibody (green) and anti-insulin antibody (red). The scale bar represents 40 μm.

E) Regulation of collectrin mRNA expression by nutritional status. Pancreatic islets of mice fasted for 24 hr (n = 3), or fed after fasting for 12 hr (n = 3) were subjected to real-time RT-PCR. Results were normalized to the level of TBP mRNA. Data are the mean ± SEM. *$p < 0.05$.

F) Increased collectrin expression in islets from obese HF mice. Islets were isolated from HF (implemented for 15 weeks) obese mice (n = 3) and their lean controls (n = 3) for real-time RT-PCR and Western blotting. Results of real-time RT-PCR were normalized for the level of TBP mRNA. Data are the mean ± SEM. *$p < 0.05$.

G) Increased collectrin mRNA expression in islets from KKAy mice. Islets were isolated from 13-week-old KKAy mice (n = 5) and their lean controls (n = 5) for real-time RT-PCR. Results were normalized for the level of TBP mRNA. Data are the mean ± SEM. *$p < 0.05$.

(pcDNA3.1-myc-collectrin) or empty vector into INS-1 cells. The level of exogenous collectrin mRNA expression in the stable clones (collectrin-INS-1 cells) was 3.1- to 4.3-fold greater compared to that in stable clones transfected with empty vector (Figure 3A). The effect of overexpression of collectrin on insulin secretion was assessed (Figure 3B). Collectrin-INS-1 cells (5 independent clones) and control clones transfected with empty vector (5 clones) were incubated for 30 min with 2.2 to 22.2 mM glucose. Insulin secretion from collectrin-INS-1 cells was significantly increased at stimulatory glucose concentrations (5.5-22.2 mM) compared with that from control cells, whereas there was no difference at 2.2 mM glucose. The increase of insulin secretion was not due to altered insulin synthesis, since the insulin content of collectrin-INS-1 cells and control cells was similar (Figure 3C). We then suppressed the expression of endogenous collectrin in INS-1 and MIN6 cells by small inhibitory RNA (siRNA) (Figure 3D). Suppression of endogenous collectrin led to 39% (INS-1) and 44% (MIN6) decrease in the expression of collectrin, while insulin secretion stimulated by 22.2 mM glucose was significantly inhibited by 25% in INS-1 cells and 33% in MIN6 cells. These results suggest that collectrin has an important role in enhancing glucose-stimulated insulin secretion.

In β cells, an increase of the ATP/ADP ratio due to glucose metabolism closes ATP-sensitive potassium channels, leading to membrane depolarization, calcium influx, fusion of insulin-containing secretory granules with the plasma membrane, and

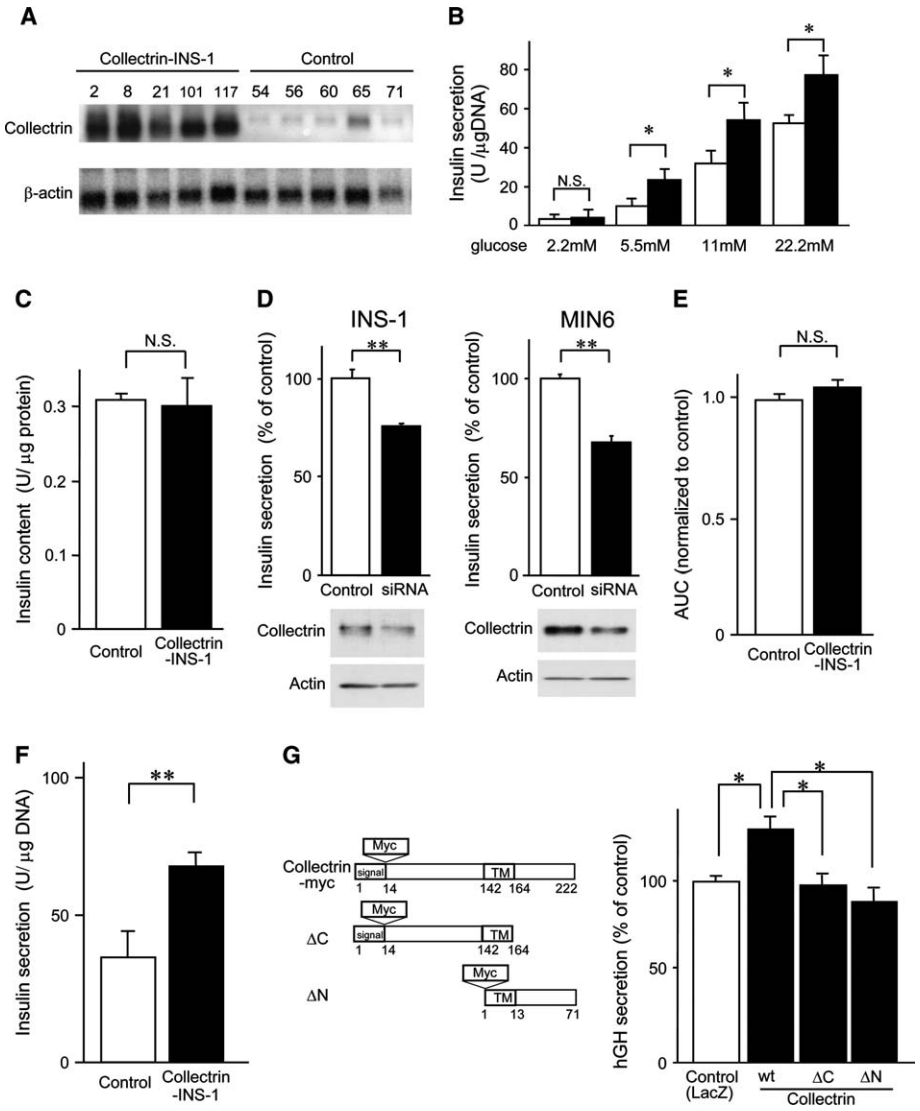

Figure 3. Collectrin augments insulin secretion by INS-1 cells

A) Northern blotting analysis of collectrin expression in stable clones. INS-1 cells were transfected with pcDNA3.1-myc-collectrin or the empty pcDNA3.1 vector. Ten stable clones (collectrin-INS-1 clones 2, 8, 21, 101, and 117; vector control clones 54, 56, 60, 65, and 71) were obtained. The gels were scanned and quantified.

B) Glucose-stimulated insulin secretion from collectrin-INS-1 cells (clones 2, 8, 21, 101, and 117) (solid bars) and control INS-1 cells (54, 56, 60, 65, and 71) (open bars). Insulin secretion was assessed in triplicate for each clone. Data are the mean ± SEM. N.S., not significant. *$p < 0.05$ compared with control INS-1 cells.

C) Insulin content of collectrin-INS-1 cells and control INS-1 cells. Collectrin-INS-1 cells (5 clones) and INS-1 cells (5 clones) were plated on 6-well plates at a density of 5×10^5 cells. Insulin content was measured in triplicate for each clone. Data are the mean ± SEM. N.S., not significant.

D) Suppression of collectrin expression by siRNA reduces glucose-stimulated insulin secretion. INS-1 and MIN6 cells were transfected with specific rat and mouse collectrin siRNA or control siRNA. Expression of endogenous collectrin was determined by Western blotting. The secretory response of insulin to glucose was reduced by collectrin-specific siRNA. Data are the mean ± SEM. **$p < 0.01$ compared with the control.

E) Changes of the $[Ca^{2+}]_i$ in response to 27.8 mM glucose and 20 mM KCl in collectrin-INS-1 cells (clone 2) and control INS-1 cells (clone 60). There is no significant difference of the area under the curve (AUC) for clone 2 and clone 60. Data are the mean ± SEM.

F) Insulin secretion in response to 60 mM KCl. High K^+-induced insulin secretion was significantly greater in collectrin-INS-1 cells (5 clones) compared with control cells (5 clones). Insulin secretion was tested in triplicate for each clone. Data are the mean ± SEM. *$p < 0.05$.

G) Effect of collectrin on glucose-stimulated secretion of growth hormone from INS-1 cells. INS-1 cells were transfected with LacZ, Wt-collectrin, or mutant-collectrin (0.5 μg) and pcDNA3-hGH (0.5 μg). Values are shown as the percentage of growth hormone secretion relative to that in control cells (LacZ). Data are the mean ± SEM. *$p < 0.05$.

the secretion of insulin (Wollheim, 2000, Rorsman & Renström, 2003). To determine how collectrin enhances insulin secretion, we first measured $[Ca^{2+}]_i$ in collectrin-INS-1 clones and control clones. Glucose stimulation lead to a similar increase of $[Ca^{2+}]_i$ in both types of cells (Figure 3E). The similar response of $[Ca^{2+}]_i$ suggested that collectrin acts on steps beyond Ca^{2+} influx in the process of insulin secretion. High K^+-induced depolarization evokes Ca^{2+}-dependent insulin release from β cells. Like glucose, KCl stimulated insulin secretion was more pronounced in collectrin-INS-1 cells than in control cells (Figure 3F). Pancreatic β cells contain at least three functionally distinguishable pools of insulin granules: undocked, docked, and primed readily releasable pool (RRP) (Reviewed in Rorsman and Renström, 2003). Because the amount of exocytosis induced by K^+ stimulation is considered to represent the size of the RRP (Reviewed in Rorsman and Renström, 2003), the enhanced response to K^+ stimulation suggested that overexpression of collectrin may increase the size of the RRP.

The role of collectrin in the exocytotic pathway was further explored by transiently cotransfecting INS-1 cells with WT-collectrin, deletion mutants of collectrin (ΔC-, and ΔN-collectrin), or LacZ expression vector together with human growth hormone (hGH) expression vector (Figure 3G, left panel). In transfected cells, hGH is targeted to insulin-containing secretory granules, and the hormone allows the monitoring of the exocytotic process (Coppola et al., 1999; Iezzi et al., 2000). Transfection of WT-collectrin significantly increased glucose-stimulated hGH secretion compared with that of LacZ. However, augmented hGH secretion was not observed when mutant collectrin was transfected into the cells (Figure 3G, right panel). These results emphasize the role of collectrin in the process of exocytosis in INS-1 cells.

Collectrin is located on the limiting membrane of insulin granules

We next investigated the subcellular distribution of collectrin in collectrin-INS-1 cells. Immunofluorescence microscopy showed that collectrin was localized in the cytoplasm of INS-1 cells. Double staining for collectrin and insulin showed that both signals were often colocalized in the cells (Figure 4A). To

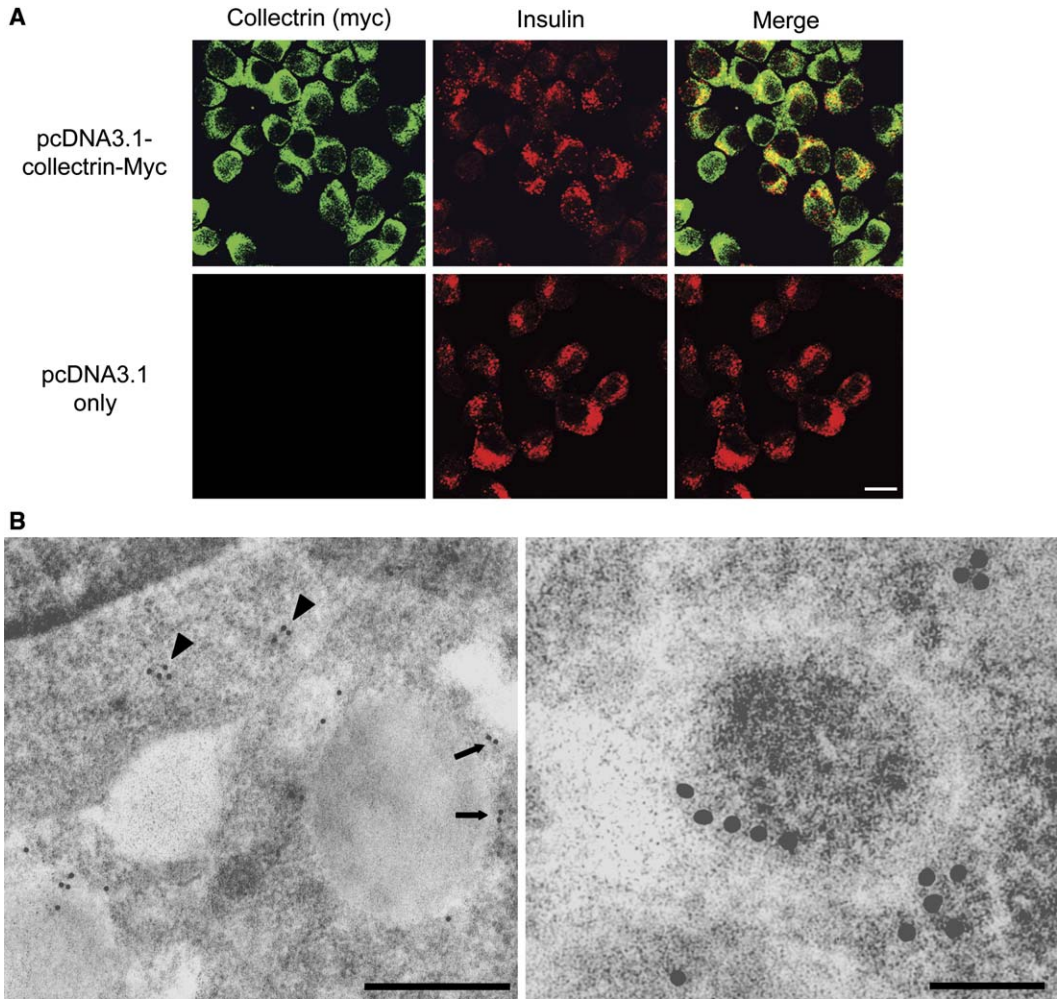

Figure 4. Intracellular localization of collectrin in INS-1 cells

A) Intracellular localization of myc-tagged collectrin. Collectrin-INS-1 (upper panels) and control INS-1 cells (lower panels) were double stained with an anti-insulin antibody (Alexa 594 label, red) and an anti-myc antibody (Alexa 488 label, green) for examination by confocal microscopy. The scale bar represents 5 μm.

B) Ultrathin sections of INS-1 cells were immunolabeled with a rabbit antibody for collectrin. Gold particles were found on the periphery of insulin granules (arrow) as well as microvesicles (arrowhead). The scale bars represent 500 nm (left) and 100 nm (right).

substantiate the findings in light microscopy, we performed immunogold electron microscopy. When ultrathin sections of INS-1 cells were immunolabeled with anti-collectrin antibody, immunogold particles were found on the periphery of large secretory granules as well as microvesicles (Figure 4B). This indicates the localization of collectrin to the limiting membrane of insulin granules.

Collectrin increases insulin exocytosis in vivo

The following experiments assessed the role of collectrin in insulin secretion in vivo. We generated transgenic mice with β cell targeted overexpression of collectrin (RIP-collectrin Tg). Collectrin protein in the pancreatic islets of the transgenic mice was 2.3-fold elevated relative to endogenous collectrin by Western blotting (Figure 5A). The body weight and random blood glucose levels did not differ between RIP-collectrin Tg mice and control mice (data not shown). However, glucose tolerance tests (GTT) revealed that blood glucose levels were significantly lower in the Tg mice than in controls at 30 min, 60 min, and 120 min after a glucose load (Figure 5B). The acute phase of insulin secretion (15 min after glucose load) was significantly increased by 1.6-fold in Tg mice (Tg: 781.5 ± 79.1 pg/ml; control: 496.1 ± 131.1 pg/ml, $p < 0.05$) (Figure 5C). Immunostaining of pancreatic sections with an antibody against insulin revealed a normal islet architecture in the RIP-collectrin Tg mice (Figure 5D). Likewise, there was no significant difference in the β cell area per pancreas between Tg and control mice as revealed by quantitative analysis (Figure 5D). In agreement with the results obtained in INS-1 cells, the insulin response to high glucose was increased in collectrin-Tg islets (Figure 5E). Cumulative glucose-induced insulin secretion from RIP-collectrin Tg islets was significantly augmented by 2.8-fold at 30 min compared with control islets (Figure 5E).

To investigate the mechanism underlying the increase in glucose-stimulated insulin secretion by collectrin-Tg islets, we directly measured the exocytosis of insulin granules and the rise in cytosolic Ca^{2+} in response to glucose stimulation by 2-photon excitation imaging. This novel morphological technique enables the precise monitoring of individual exocytotic events and other relevant parameters in a defined area, of intact islets (Takahashi

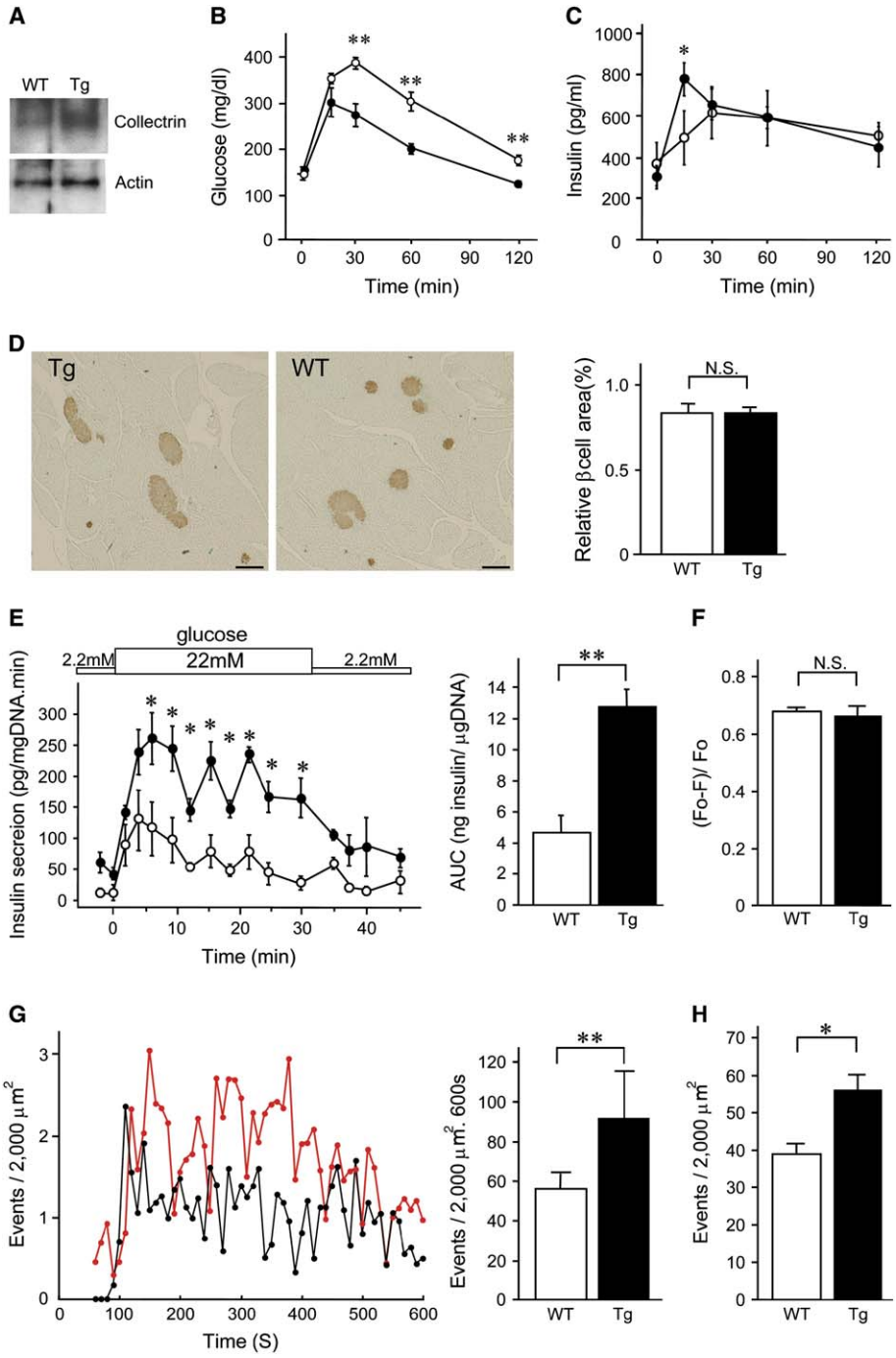

Figure 5. Collectrin increases insulin exocytosis in vivo

A) Generation of transgenic mice overexpressing collectrin in β cells (RIP-collectrin Tg). Expression of collectrin in the islets of Tg mice caused a 2.3-fold increase compared with the islets of control mice.

B and C) Glucose-stimulated insulin secretion in RIP-collectrin Tg mice. Blood glucose levels in Tg mice (closed circles: n = 5) at 30, 60, and 120 min after a glucose load were significantly lower than in control mice (open circles: n = 5) (**B**) The serum insulin level of Tg mice at 15 min after a glucose load was significantly increased compared with control mice (**C**). Data are the mean ± SEM. *p < 0.05, **p < 0.01.

D) Immunostaining of pancreatic sections from 20- to 24-week-old Tg and control mice. The β cell area is shown as a percentage of the total pancreatic area. Data are the mean ± SEM for 3 mice. The scale bar represents 100 μm.

E) Insulin secretory response to glucose in perifused islets of Tg mice. The insulin response to 22 mM glucose was significantly increased in Tg islets. Total insulin secretion from perifused isolated Tg islets and control islets was calculated from the area under the curve (AUC) (right). Data represent the mean ± SEM of three experiments on each genotype. *p < 0.05.

F) Response of $[Ca^{2+}]_i$ to glucose in Tg islets. Changes of $[Ca^{2+}]_i$ in response to 20 mM glucose were measured in islets with fura-2 using two-photon excitation imaging in pancreatic β cells and represented as $(F_0\text{-}F)/F_0$, where F_0 and F represent resting fluorescence and the fluorescence after stimulation, respectively. The $(F_0\text{-}F)/F_0$ response to glucose stimulation was calculated and the mean ± SEM is presented.

G) Exocytosis in response to 20 mM glucose. Exocytosis from Tg islets (n = 5, red) and control islets (n = 5, black) was detected with 2-photon microscopy. Data are the mean ± SEM. **p < 0.01.

H) Exocytosis evoked by photolysis of the caged-Ca^{2+} compound. Data represent the mean ± SEM of 4 experiments on each genotype. *p < 0.05.

et al., 2002; Kasai et al., 2005). The glucose-induced increase of Ca^{2+} measured with Fura-2 was similar in collectrin-Tg mice and control mice (Figure 5F). When the number of exocytotic events was visualized with a solution containing a fluid-phase tracer (sulforhodamine B), exocytotic events during a period of 10 min of 20 mM glucose stimulation were significantly increased in RIP-collectrin Tg islets (Tg: 91.7 ± 23.1 events/2,000 μm^2; control: 55.7 ± 7.1 events/2,000 μm^2, $p < 0.01$) (Figure 5G). We also directly examined the role of collectrin in Ca^{2+}-dependent insulin exocytosis by photolysis of a caged-Ca^{2+} compound (NP-EGTA). Uncaging leads to a large, spatially homogenous and rapid increase in $[Ca^{2+}]_i$ in the islets as well as triggering insulin exocytosis (Takahashi et al., 2004). We found that insulin exocytosis evoked by photolysis of the caged-Ca^{2+} compound was also increased in Tg islets (Figure 5H). Taken together, these results clearly demonstrate that collectrin increases insulin secretion by enhancing exocytosis.

Collectrin increases exocytosis by interaction with snapin

To further elucidate the molecular relationship between collectrin and exocytosis, we searched for a molecule that interacts with collectrin by yeast two-hybrid screening using collectrin as the bait. After screening more than 10^7 independent clones,

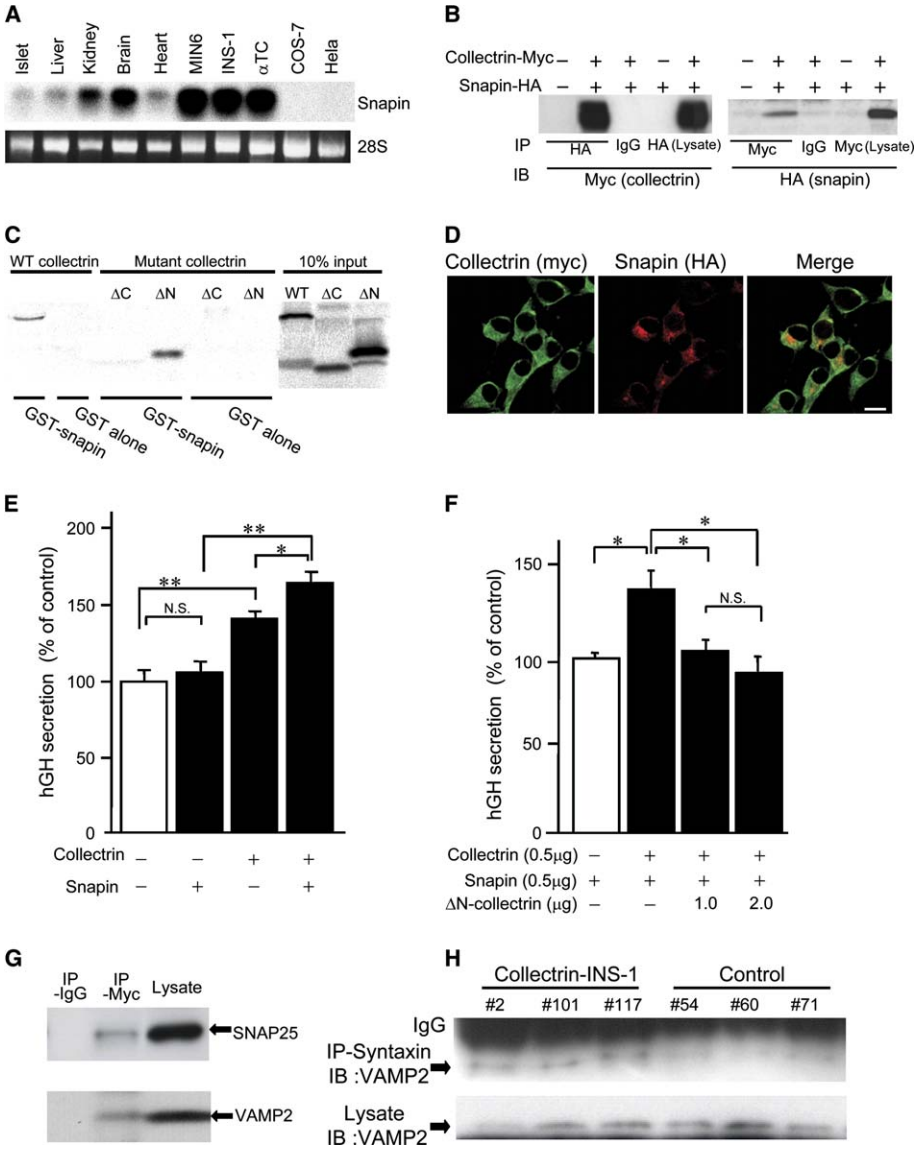

Figure 6. Effect of interaction between collectrin and snapin on exocytosis

A) Northern blotting analysis of snapin gene expression.

B) Interaction of collectrin with snapin in vivo. pcDNA3.1-myc-collectrin and/or pcDNA3.1-HA-snapin expression vectors were cotransfected into HEK 293 cells. The interaction was evaluated by immunoprecipitation with anti-HA antibody or anti-myc antibody, followed by immunoblotting.

C) Interaction of collectrin in vitro. WT-collectrin, ΔN-collectrin, or ΔC-collectrin was translated in vitro and labeled with ^{35}S. Binding of collectrin to GST-snapin or GST alone was evaluated.

D) Intracellular localization of HA-tagged snapin. Collectrin-INS-1 cells were transfected with pcDNA3.1-HA-snapin. Cells were double-stained with anti-HA antibody (Alexa 594 label, red) and anti-myc antibody (Alexa 488 label, green). The scale bar represents 5 μm.

E and F) Influence of functional interaction between collectrin and snapin on glucose-stimulated secretion of growth hormone. INS-1 cells were transfected with collectrin (0.5 μg) or snapin (0.5 μg) expression vector plus pcDNA3-hGH (0.5 μg) (n = 10). The total amount of DNA was adjusted to 1.5 μg (E) and 3.5 μg (F) using pcDNA3.1-lacZ. INS-1 cells were transfected with the WT or ΔN collectrin and snapin expression vectors plus pcDNA3-hGH (n = 3) (F). Values show the percentage of growth hormone secretion relative to control. Data are the mean ± SEM. NS: not significant, *$p < 0.05$, **$p < 0.01$.

G) Coimmunoprecipitation of collectrin with SNAP-25, VAMP2, and syntaxin 1. Collectin-INS-1 cell lysates were immunoprecipitated with anti-myc antibody. SNAP-25, VAMP2, and syntaxin 1 were detected by immunoblotting.

H) Effect of collectrin on SNARE complex formation. Lysates of collectrin-INS-1 cells or control INS-1 cells were immunoprecipitated with an anti-syntaxin 1 antibody and the amount of VAMP2 bound to syntaxin 1 was determined by immunoblotting with an anti-VAMP2 antibody. Association of syntaxin 1 with VAMP2 is increased in collectrin-INS-1 cells.

we found 7 clones that strongly interacted with collectrin in yeast, among these, 3 clones encoded snapin. Snapin is a 15 kDa protein containing the predicted coiled-coil domain in the C-terminal half (Ilardi et al., 1999). Snapin has been reported to bind to synaptic soluble N-ethylmaleimide-sensitive-factor attachment protein receptor (SNARE) complexes (reviewed in Chen and Scheller, 2001; Jahn et al., 2003). Through direct interaction with SNAP-25, snapin is implicated in calcium-triggered vesicle fusion by regulating the association between the SNARE complex and the putative Ca^{2+}-sensor synaptotagmin (Ilardi et al., 1999). Although snapin was initially regarded as a brain-specific molecule (Ilardi et al., 1999), subsequent studies have revealed its ubiquitous expression (Buxton et al., 2003). Northern blotting analysis showed that snapin mRNA was also expressed in pancreatic islets, as well as MIN6 and INS-1 cells (Figure 6A).

Subsequently we evaluated the specificity of the interaction between collectrin and snapin both in vivo and in vitro. As shown in Figure 6B, HA-snapin was able to coimmunoprecipitate myc-collectrin and conversely myc-collectrin also associated with HA-snapin in 293 cells. A direct interaction between collectrin and snapin was verified by the GST-pull-down assay. GST-snapin bound to WT-collectrin and ΔN mutant collectrin, but not to ΔC mutant collectrin (Figure 6C), indicating direct binding of snapin to the C-terminal domain of collectrin. Next, collectrin-INS-1 cells were transfected with HA-tagged snapin expression vector and the intracellular localization of snapin was investigated by immunofluorescence microscopy using anti-HA antibody. Double staining for collectrin and snapin revealed that both signals were frequently colocalized in the cytoplasm of INS-1 cells (Figure 6D).

To investigate the functional relevance of this interaction, INS-1 cells were transiently transfected with collectrin and/or snapin expression vectors together with the hGH expression vector, after which glucose-stimulated hGH secretion was measured (Figure 6E). Snapin alone did not increase hGH secretion, while cotransfection of collectrin and snapin significantly augmented hGH release (Figure 6E). Although ΔN-collectrin binds to snapin, the mutant did not augment glucose-stimulated hGH secretion (Figures 6C and 3G). Cotransfection of ΔN-collectrin

significantly suppressed the augmented hGH secretion by collectrin and snapin (Figure 6F). These results strongly suggest that collectrin is implicated in exocytosis by interacting with snapin.

We next investigated whether collectrin was able to bind to the SNARE complex. Lysates from collectrin-INS-1 cells were subjected to immunoprecipitation using anti-myc antibody, after which the precipitates were immunoblotted with SNAP25 and VAMP2 antibodies. As shown in Figure 6G, SNAP-25 and VAMP2 were coimmunoprecipitated with collectrin, indicating the formation of a collectrin/SNARE complex in vivo. Direct binding of collectrin to SNAP-25, syntaxin 1 and VAMP2 was subsequently examined by the GST-pull down assay. While snapin bound to GST-collectrin, SNAP-25, syntaxin 1 and VAMP2 did not (data not shown), indicating that collectrin binds to SNARE proteins indirectly, most likely by interacting with snapin. Finally, we explored the effect of collectrin overexpression on SNARE complex formation. Lysates from collectrin-INS-1 cells and control INS-1 cells were subjected to immunoprecipitation with anti-syntaxin 1 antibody and the precipitates were immunoblotted with anti-VAMP2 antibody. As shown in Figure 6H, VAMP2 immunoreactivity was increased in precipitates from collectrin-INS-1 cells relative to control cells, indicating that collectrin facilitates formation of the SNARE complex.

Discussion

Collectrin was originally discovered as a renal collecting duct-specific glycoprotein with an unknown function (Zhang et al., 2001). In the present study, we clarified that collectrin is a novel target of HNF-1 in pancreatic β cells and that it controls insulin exocytosis. In addition, we demonstrated that collectrin binds directly to snapin and forms a complex with SNARE proteins. Snapin has been suggested to potentiate the interaction of synaptotagmin with the SNARE complex during the release of synaptic vesicles (Ilardi et al., 1999). In adrenal chromaffin cells, snapin is thought to facilitate formation of the SNARE complex, which is stabilized by protein kinase A-mediated phosphorylation of snapin (Chheda et al., 2001). Although the precise role of snapin in the process of exocytosis remains unclear (Vites et al., 2004), collectrin may act in concert with snapin to increase SNARE complex formation. We found that 2.3-fold overexpression of collectrin in β cells lead to 2.8-fold enhancement of glucose-stimulated insulin secretion from perifused pancreatic islets (Figure 5E), while 39%–44% suppression of collectrin expression in insulinoma cells reduced insulin secretion by 25%–33% (Figure 3D). These results suggest an important role of collectrin in insulin secretion. Investigation of collectrin knockout mice will enhance our understanding of the physiological significance of this molecule in the process of exocytosis.

Mutations in the HNF-1α and HNF-1β genes cause MODY, which is characterized by impaired insulin secretion (Reviewed in Fajans et al., 2001). Taken together, it is possible that impaired insulin secretion in patients with MODY is due, at least in part, to reduced expression of collectrin. HNF-1α affects multiple steps during the process of glucose-stimulated insulin secretion. For example, it has been reported that GLUT2, insulin, E-cadherin and IGF-1 are target genes of HNF-1α (Pontoglio et al., 1998; Dukes et al., 1998; Wang et al., 1998, 2000; Yamagata et al., 2002; Yang et al., 2002). We do not claim that collectrin is the only target of HNF-1 in islets and it is quite possible that decreased collectrin expression alone may not explain all the phenotypes in the HNF-1α (−/−) mice. However, we believe that collectrin is one of the important players together with GLUT2, insulin, E-cadherin and IGF-1 in impaired insulin secretion in MODY3 patients. A therapeutic strategy that increases collectrin expression might be useful in MODY3 patients.

We also found that collectrin expression was enhanced in the islets of HF mice and KKAy mice. Obesity leads to the development of insulin resistance and hypersecretion of insulin by β cells. This compensatory hypersecretion of insulin not only reflects expansion of the β cell mass, but is also due to altered β cell function (Cavaghan et al., 2000). Since collectrin enhances insulin secretion, the observed increased expression in obese animals may participate in β cells adaptation to insulin resistance. It would be interesting to study the expression of collectrin in animal models with different levels of insulin resistance and diabetes mellitus. The mechanism by which collectrin expression is increased in the islets of obese mice is presently unknown. Although HNF-1α regulates transcription of the collectrin gene, expression of HNF-1α mRNA was not increased in the islets of HF mice (K.F. and K.Y., unpublished data), suggesting the existence of another regulatory mechanism. Chronic exposure of β cells to free fatty acids and hyperglycemia associated with obesity and diabetes could however contribute to the increment of collectrin expression.

In conclusion, we identified collectrin as a novel molecule that controls insulin exocytosis. Our results demonstrate that collectrin favors the formation of SNARE complexes and therefore extent the list of molecules implicated in the regulation of exocytosis. The correlation between islet expression of collectrin and insulin hyper- and hypo-secretory states emphasizes the key role of collectrin in β cell function. Consequently, collectrin may be a potential target for the treatment of diabetes associated with impaired insulin secretion.

Experimental procedures

Suppression subtraction hybridization and differential screening

INS-1 cells overexpressing the dominant negative mutant P291fsinsC-HNF-1α under control of the reverse tetracycline-dependent transactivator (HNF1α-P291fsinsC#32) have been described previously (Wang et al., 2000). Total RNA was prepared using Trizol reagent (Invitrogen, San Diego, CA) and poly(A)$^+$ mRNA was subsequently isolated with a poly(A) RNA isolation kit (Qiagen, Hilden, Germany). Suppression subtraction hybridization (SSH) was performed using a PCR Select cDNA Subtraction Kit (BD Biosciences Clontech) according to the protocol of the manufacturer. Driver cDNA was synthesized from the mRNA of HNF1α-P291fsinsC#32 cells induced with doxycycline for 48 hr and tester cDNA was synthesized from the mRNA of uninduced HNF1α-P291fsinsC#32 cells. The subtracted cDNAs were inserted into the pGEM-T Easy vector (Promega, Madison, WI) and transformed into *Escherichia coli* DH5α to yield an SSH library. A PCR-Select Differential Screening Kit (Clontech Laboratories, Palo Alto, CA) was used to screen the differentially expressed products according to the instructions of the manufacturer.

Cloning of the 5′-flanking promoter region of rat collectrin

The 5′-flanking promoter region of the rat collectrin gene was cloned with a Genome Walker Kit (Clontech) according to the protocol of the manufacturer using the following primers: 5′-TCATCGGGCACCTGGACACTTTC AC-3′ and 5′-GTTCTGTTGATTCAGCTGGCTTTTC-3′.

Reporter gene analysis

The human collectrin promoter containing a putative HNF-1 binding site was amplified by PCR with the forward primer 5′-GACAGGACTCAGATCTTC CCATCA-3′ (underlined nucleotides indicate the cloned *Bgl*II site) and the

reverse primer 5′-CAACATTCTTTCAAGCTTGAAAAC-3′ (underlined nucleotides indicate the cloned *Hind*III site). The PCR products were subcloned into the pGL3 basic reporter vector (Promega) to generate pGL3-collectrin. The HNF-1α–binding site (5-GTTAATCATTAA-3) was altered to 5-GTTGGCTAC CAG-3 by PCR. INS-1 cells were transfected for 3 hr in OPTI-MEMI (Life Technologies, Rockville, MD) with the indicated amounts of expression vectors and the reporter gene (as described in the figure legend) together with pRL-TK (the internal control) using Lipofectamine PLUS reagent (Life Technologies) as described previously (Yamagata et al., 1998).

Electrophoretic mobility shift assay

The pcDNA3.1-WT-HNF-1α or pcDNA3.1-WT-HNF-1β expression vector (Yoshiuchi et al., 2002) was transfected into HeLa cells and nuclear protein was extracted. Then 2 μg of protein was incubated with a ^{32}P-labeled oligonucleotide containing the HNF-1 binding site of the human collectrin gene (5′-GATGGGTGTTAATCATTAAACCTTT-3′). The DNA-protein complexes were separated by 5% polyacrylamide gel electrophoresis.

Northern blotting and real-time RT-PCR

Northern blotting was carried out as described previously (Iwahashi et al., 2002). For real-time quantitative PCR, pancreatic islets were isolated as described previously (Yamagata et al., 2002) and total RNA was extracted. Collectrin cDNA was synthesized from the total RNA and was tested in triplicate with an ABI PRISM 7900 (Applied Biosystems, Foster City, CA) using the following specific primers and a fluorescence-labeled probe: 5′-ATTCGGTGTG ATATTTTGCATTGT-3′, 5′-TCCAGGTGGTCCTTTGTTGTT-3′, and 5′-(FAM)-TCCGGCAACGCAGAA-3′. The primers and the probe for the TATA box binding protein (TBP) (endogenous control) were purchased from ABI.

Human pancreatic tissue, laser capture microdissection, and microarray analysis

Human pancreases from four donors were obtained from the New England Organ Bank (NEOB) with informed consent to use for research and were processed in the Islet Cell Resource Center of the Joslin Diabetes Center. After trimming away excess fat and connective tissue, small pieces of pancreas were excised, placed in cryomolds, embedded in Tissue-Tek OCT medium (Sakura Finetek U.S.A., Torrance, CA), immediately frozen in chilled isopentane, and stored at −80ºC. Frozen pancreas tissues were sectioned at 8 μm in a cryostat, mounted on uncoated glass slides (Fisher Scientific, Pittsburg, PA), and stored at −80ºC until the microdissection.

Laser Capture Microdissection (LCM) was performed as described previously. The frozen pancreatic sections were dehydrated completely air-dried and LCM was performed using PixCell II Laser Capture Microdissection System (Arcturus Engineering, Mountain View, CA). Laser capture was performed under direct microscopic visualization by melting of selected cells onto a thermoplastic film mounted on optically transparent LCM caps (Arcturus). The β cell rich tissue was identified by its autofluorescence. Total RNA was extracted from microdissected samples using the PicoPure RNA Isolation Kit (Arcturus). Genomic DNA contamination was removed by incubation with 14 units of DNase I for 15 min at room temperature (RNase Free DNase Set, Qiagen). After extraction total RNA was amplified using the RiboAmp HS RNA Amplification Kit (Arcturus). Amplified RNA (1.5 μg) obtained from each sample was converted into double-stranded cDNA using the RiboAmp HS RNA Amplification Kit (Arcturus). Double stranded cDNA products were purified by filtering through the MiraCol™ Purification Columns (Arcturus). Biotinylated cRNA was generated from purified cDNA samples by in vitro transcription reaction using a BioArray High Yield RNA Transcript Labeling Kit (Enzo Diagnostics, Farmingdale, NY). RNA products were then purified using the MiraCol™ Purification Columns (Arcturus) and fragmented to nucleotide stretches of 30-200 nucleotides. The biotinylated fragmented RNA was hybridized to GeneChip Human X3P Array (Affymetrix, Santa Clara, CA). After hybridization the chips were washed in a GeneChip Fluidics Station 400 (Affymetrix) and stained with streptavidin-phycoerythrin, the signal was amplified by biotinylated anti-streptavidin and analyzed by a GeneChip Scanner 3000 using the GeneChip Operating Software (GCOS) (Affymetrix). The array data were normalized using the DNA-Chip Analyzer (dChip) software. The program performs a model-based expression analysis that allows probe-level analysis on multiple arrays and normalizes the array data to a common baseline array having the median overall brightness, as measured by the median CEL intensity in an array (Li and Wong, 2001).

Immunoblotting, immunohistochemistry, and immunofluorescence studies

Rabbit anti-collectrin antibody was raised against a synthetic peptide (NDAFMTEDERLTPL) corresponding to amino acids 209 to 222 of human collectrin. Western blotting analysis and immunohistochemistry were performed as described previously (Yamagata et al., 2002). Guinea pig anti-porcine insulin antibody (1:5,000) (Dako Corporation, CA) and rabbit anti-collectrin antibody (1:200) were used as the primary antibodies. Human pancreatic sections were obtained from SuperBio Chips (Seoul, Korea). For the deglycosylation of glycoproteins, proteins were treated with N-glycosidase F (Roche, IN) and O-glycosidase (Roche) before Western blotting according to the manufacturer's instructions. For the immunofluorescence study, INS-1 cells were grown on Lab-Tek II chamber slides (Nunc-Immuno Plate, Roskilde, Denmark) for 72 hr. Then the cells were fixed in 4% paraformaldehyde and permeabilized with 0.1% Triton X-100 in phosphate-buffered saline containing 1% bovine serum albumin (BSA). Guinea pig anti-porcine insulin antibody (1:100), mouse anti-myc antibody (1:200) (Medical Bioscience Laboratories), and rabbit anti-HA antibody (1:200) (Medical Bioscience Laboratories) were used as the primary antibodies. Immunofluorescence was viewed under a laser scanning confocal microscope (LSM510; Carl Zeiss, Eching, Germany).

Generation of stable INS-1 cell lines overexpressing collectrin

The nucleotide sequence encoding the myc epitope was introduced into human collectrin cDNA in frame after the signal sequence by PCR. INS-1 cells were transfected with the pcDNA3.1-myc-collectrin expression plasmid or empty vector using Lipofectamine PLUS reagent. Stable transformants (collectrin-INS-1 cells) were obtained by cloning the colonies under selection with 400 μg/ml neomycin (Sigma-Aldrich, St. Louis, MO).

Insulin secretion and cellular insulin content

Insulin secretion from INS-1 cells was measured over a period of 30 min, in Krebs-Ringer- bicarbonate-4-(2-hydroxyethyl)-1-piperazine ethanesulfonic acid (HEPES) buffer (KRBH; 140 mM NaCl, 3.6 mM KCl, 0.5 mM NaH_2PO_4, 0.5 mM $MgSO_4$, 1.5 mM $CaCl_2$, 2 mM $NaHCO_3$, 10 mM HEPES, and 0.1% BSA), containing the indicated stimulators. The insulin content was determined after extraction with acid ethanol as described previously (Yamagata et al., 2002). Insulin was detected by using a Glazyme insulin enzyme immunoassay kit (Wako Pure Chemical Industries, Osaka, Japan).

SiRNA knockdown of collectrin expression

For siRNA-mediated knockdown of collectrin expression, nucleotides 229-253 (GenBank AF178086) of rat collectrin cDNA (5′-GCAAUGUAACCCAGA GAGUGUCAUU-3′) and nucleotides 344-368 (GenBank AF178085) of mouse collectrin cDNA (5′-GGUCACGGACCCUUCCAACAAUUAU-3′) were used as the target sequences. Transfection of siRNA (50 nM) into INS-1 cells and MIN6 cells was performed by using RNAiFect reagent (Qiagen) according to the protocol of the manufacturer. The following sequences were used as control siRNA: 5′-GGUCACGGACCCUUCCAACAAUUAUdTdT-3′ for mouse collectrin and 5′-GCAAAUGACCCAGAGUGUGCUAAUUdTdT-3′ for rat collectrin. SiRNA duplex was synthesized by Invitrogen. After incubation for 48 hr, Western blotting and insulin secretion experiments were performed as described above.

Measurement of the intracellular calcium concentration

INS-1 cells were cultured on glass-bottomed culture dishes (MatTek) for 2 days. Subsequently, the cells were loaded with 2 μM Fura-2 acetoxymethyl ester (Dojin Chemicals Co., Kumamoto, Japan) for 60 min at 37ºC. Changes of $[Ca^{2+}]_i$ were determined as the ratio of emitted light intensity (detected at 510 nm) after excitation at either 340 or 380 nm.

Growth hormone secretion assay

Mutant collectrin cDNA was generated by PCR and subcloned into pcDNA3.1. To construct N-terminal (ΔN-collectrin) and C-terminal (ΔC-collectrin) deletion mutants, the following primers were used (ΔN: 5′-GGATCC ATG*GAACAAAAACTCATCTCAGAAGAGGATCTG*CCCATCTGGATTATTA TATTTGGT-3′ and 5′-GAATTCTCAGAGAGGGGTGAGCCTCTCATC-3′, ΔC: 5′-GGATCCATGTTGTGGCTGCTCTTTTTTCTG-3′ and 5′-GAATTCCTAGAT CCCTGATAAAATCAGTAGTGC-3′ (the underlined nucleotides indicate the cloning sites and the myc tag sequence is shown in italics). INS-1 cells were cotransfected with a GH expression vector (pcDNA3-hGH),

pcDNA3.1-WT or mutant collectrin, and/or pcDNA3.1-snapin using Lipofectamine PLUS reagent. At 48 hr after transfection, cells were preincubated in glucose-free KRBH for 15 min and then incubated with KRBH containing 15 mM glucose for 30 min. GH was measured by an enzyme immunoassay kit (Roche). Secretion was expressed as the percentage of GH release into the medium relative to the total cellular GH content.

Immunoelectron microscopy

Immunoelectron microscopy was performed as described previously (Wada and Kanwar, 1998). INS-1 cells were fixed with 0.1% paraformaldehyde and 0.05% glutaraldehyde in 0.01 M phosphate buffer (pH 7.4) for 30 min. After the cells were scraped off the dish, a pellet was prepared with a Microfuge. Then the pellet was dehydrated in a graded ethanol series and its temperature was gradually lowered to −20ºC. Stepwise infiltration was carried out with Lowicryl-K4 medium and the cells were finally embedded in this low temperature polymer resin. Uniform polymerization was carried out using ultraviolet light at a temperature below −20ºC for 24 hr and then at room temperature for 48 hr. Approximately 60-nm sections were picked up on 300 mesh nickel grids. The sections were pretreated with 20 mM Tris-buffered saline (pH 8.2) containing 0.25% bovine serum albumin, incubated with anti-collectrin antibody, and then incubated with an anti-rabbit IgG conjugated with 15 nm colloidal gold particles for 4 hr at room temperature. The sections were washed with Tris-buffered saline, stained with lead citrate and uranyl acetate, and examined under an electron microscope at an accelerating voltage of 75 kV.

RIP-collectrin transgenic mice

Human myc-tagged collectrin cDNA was ligated to the rat insulin II promoter containing the expression vector (Yamagata et al., 2002) and a 1.7-kb HindIII expression unit was microinjected into the fertilized eggs of C57BL6 mice. Age- and sex-matched transgene-negative littermates were used as controls. For the glucose tolerance test, 24- to 28-week-old male mice were fasted for 16 hr and then injected intraperitoneally with glucose (2 g/kg). For perifusion experiments, 20 islets were perifused with Hepes-Krebs buffer containing 0.5% BSA at a flow rate of 1 ml/min. The experimental protocol was approved by the Ethics Review Committee for Animal Experimentation of Osaka University.

Two-photon excitation imaging of exocytosis in pancreatic islets

Exocytosis of insulin granules was visualized in living pancreatic islets with a solution containing a fluid-phase tracer (sulforhodamine B at 0.7 mM) and 2-photon excitation imaging, as described previously (Takahashi et al., 2002). To trigger the exocytosis of insulin by photolysis of a caged-Ca^{2+} compound, islets were preincubated for 30 min at 37ºC in serum-free DMEM containing 10 μM fura-2FF-AM (Tef Lab), 25 μM NP-EGTA-AM (Molecular Probes), 0.03% crempho EL (Molecular probes), and 0.1% BSA (Takahashi et al., 2004). Photolysis of NP-EGTA was induced with a brief flash (0.2-0.5 s) of a mercury lamp. Exocytosis in response to 20 mM glucose or uncaging of NP-EGTA was measured within an arbitrary area (2,000 μm^2) of the islets.

Yeast two-hybrid screening

The collectrin cDNA postsignaling sequence was subcloned in-frame into the pGBKT7 bait vector (BD Biosciences Clontech) and transformed to yeast AH109 (BD Biosciences Clontech). AH109 yeast was then mated at 30ºC for 24 hr with Y187yeast that had been pretransformed with a human kidney cDNA library (BD Biosciences Clontech). The mated yeasts were plated on selection plates (SD/-Ade/-His/-Leu/-Trp) containing 2.5 mM 3-amino-1, 2, 4-triazole (3-AT). After 7-10 days, robust growing clones were picked up and DNA was extracted. The DNA was transformed into Y187 yeast and mated with AH109-collectrin again to confirm the interaction.

Immunoprecipitation and GST pull-down assay

Myc-tagged collectrin and HA-tagged snapin expression vectors were cotransfected into 293 cells for 48 hr and the cells were lysed in a lysis buffer containing 20 mM Tris-HCl (pH 7.5), 5 mM ethylenediaminetetraacetic acid (EDTA), 10 mM $Na_4P_2O_7$, 100 mM NaF, 2 mM Na_3VO_4, 1% NP-40, 1 mM phenylmethylsulfonylfluoride (PMSF), 10 μg/ml aprotinin, and 10 μg/ml leupeptin. The lysates were preincubated with protein G–Sepharose (Amersham Biosciences) for 60 min and then incubated overnight with an anti-myc mouse monoclonal antibody (9B11, Cell Signaling Technology, Beverly, MA), anti-HA rabbit polyclonal antibody (Medical and Biological Laboratories, Nagoya, Japan), or nonimmune serum at 4ºC. Immunoprecipitates were captured with 5% (v/v) protein G–Sepharose for 60 min and washed in the lysis buffer. Then the immunoprecipitates were solubilized with sample buffer and subjected to sodium dodecyl sulfate-polyacrylamide gel electrophoresis.

Full-length human collectrin and snapin cDNAs were generated by PCR and cloned in-frame in the pGEX4T3 vector (Amersham). GST fusion proteins were expressed and purified from *E. coli* BL21 (DE3). ^{35}S-labeled syntaxin 1, SNAP-25, VAMP2, collectrin, and snapin were synthesized using TNT quick coupled transcription/ translation systems. Then the GST pull-down assay was performed as described previously (Nishizawa et al. 2002).

Statistical analysis

All results were expressed as the mean ± SEM. Differences between groups were examined for statistical significance using Student's *t*- test and $p < 0.05$ was taken to indicate a significant difference.

Supplemental data

Supplemental Data include one figure, Supplemental Experimental Procedures, and Supplemental References and can be found with this article online at http://www.cellmetabolism.org/cgi/content/full/2/6/373/DC1/.

Acknowledgments

We thank Ms. F. Katsube and Dr. A. Ihara for their valuable help with this study. We also thank Dr. R. Palmiter (University of Washington) for providing the RIP expression vector, Dr. J. Miyazaki (Osaka University) for the gift of MIN6 cells, and Dr. J.M. Zabolotny (Beth Israel Deaconess Medical Center) for critical reading of the manuscript. This work was supported by grants from the Ministry of Education, Culture, Sports, Science, and Technology of Japan. The work of Drs. L.M. and G.C.W. was supported by grants from the National Institute of Health (NIH NCRR ICR U4Z RR 16606 and U19DK61251) and the Diabetes Research and Wellness Foundation. Drs C.B.W. and H.W. were supported by the Swiss National Science Foundation No 32-66907.01 and 32-66907.02.

Received: November 16, 2004
Revised: August 13, 2005
Accepted: November 3, 2005
Published: December 6, 2005

References

Bellanne-Chantelot, C., Chauveau, D., Gautier, J.F., Dubois-Laforgue, D., Clauin, S., Beaufils, S., Wilhelm, J.M., Boitard, C., Noel, L.H., Velho, G., and Timsit, J. (2004). Clinical spectrum associated with hepatocyte nuclear factor-1β mutations. Ann. Intern. Med. *140*, 510–517.

Buxton, P., Zhang, X.M., Walsh, B., Sriratana, A., Schenberg, I., Manickam, E., and Rowe, T. (2003). Identification and characterization of Snapin as a ubiquitously expressed SNARE-binding protein that interacts with SNAP23 in non-neuronal cells. Biochem. J. *375*, 433–440.

Cavaghan, M.K., Ehrmann, D.A., and Polonsky, K.S. (2000). Interactions between insulin resistance and insulin secretion in the development of glucose intolerance. J. Clin. Invest. *106*, 329–333.

Chen, Y.A., and Scheller, R.H. (2001). SNARE-mediated membrane fusion. Nat. Rev. Mol. Cell Biol. *2*, 98–106.

Chheda, M.G., Ashery, U., Thakur, P., Rettig, J., and Sheng, Z.H. (2001). Phosphorylation of Snapin by PKA modulates its interaction with the SNARE complex. Nat. Cell Biol. *3*, 331–338.

Coppola, T., Perret-Menoud, V., Luthi, S., Farnsworth, C.C., Glomset, J.A., and Regazzi, R. (1999). Disruption of Rab3-calmodulin interaction, but not other effector interactions, prevents Rab3 inhibition of exocytosis. EMBO J. *18*, 5885–5891.

Dukes, I.D., Sreenan, S., Roe, M.W., Levisetti, M., Zhou, Y.P., Ostrega, D., Bell, G.I., Pontoglio, M., Yaniv, M., Philipson, L., and Polonsky, K.S. (1998). Defective pancreatic β-cell glycolytic signaling in hepatocyte nuclear factor-1α-deficient mice. J. Biol. Chem. *273*, 24457–24464.

Fajans, S.S., Bell, G.I., and Polonsky, K.S. (2001). Molecular mechanisms and clinical pathophysiology of maturity-onset diabetes of the young. N. Engl. J. Med. *345*, 971–980.

Froguel, P., Zouali, H., Vionnet, N., Velho, G., Vaxillaire, M., Sun, F., Lesage, S., Stoffel, M., Takeda, J., Passa, P., et al. (1993). Familial hyperglycemia due to mutations in glucokinase: definition of a subtype of diabetes mellitus. N. Engl. J. Med. *328*, 697–702.

Horikawa, Y., Iwasaki, N., Hara, M., Furuta, H., Hinokio, Y., Cockburn, B.N., Lindner, T., Yamagata, K., Ogata, M., Tomonaga, O., et al. (1997). Mutation in hepatocyte nuclear factor-1β gene (TCF2) associated with MODY. Nat. Genet. *17*, 384–385.

Iezzi, M., Regazzi, R., and Wollheim, C.B. (2000). The Rab3-interacting molecule RIM is expressed in pancreatic β-cells and is implicated in insulin exocytosis. FEBS Lett. *474*, 66–70.

Ilardi, J.M., Mochida, S., and Sheng, Z.H. (1999). Snapin: a SNARE-associated protein implicated in synaptic transmission. Nat. Neurosci. *2*, 119–124.

Iwahashi, H., Yamagata, K., Yoshiuchi, I., Terasaki, J., Yang, Q., Fukui, K., Ihara, A., Zhu, Q., Asakura, T., Cao, Y., et al. (2002). Thyroid hormone receptor interacting protein 3 (trip3) is a novel coactivator of hepatocyte nuclear factor-4α. Diabetes *51*, 910–914.

Jahn, R., Lang, T., and Sudhof, T.C. (2003). Membrane fusion. Cell *112*, 519–533.

Kasai, K., Ohara-Imaizumi, M., Takahashi, N., Mizutani, S., Zhao, S., Kikuta, T., Kasai, H., Nagamatsu, S., Gomi, H., and Izumi, T. (2005). Rab27a mediates the tight docking of insulin granules onto the plasma membrane during glucose stimulation. J. Clin. Invest. *115*, 388–396.

Lang, J. (1999). Molecular mechanisms and regulation of insulin exocytosis as a paradigm of endocrine secretion. Eur. J. Biochem. *259*, 3–17.

Lee, Y.H., Sauer, B., and Gonzalez, F.J. (1998). Laron dwarfism and non-insulin-dependent diabetes mellitus in the Hnf-1alpha knockout mouse. Mol. Cell. Biol. *18*, 3059–3068.

Li, C., and Wong, W.H. (2001). Model-based analysis of oligonucleotide arrays: expression index computation and outlier detection. Proc. Natl. Acad. Sci. USA *98*, 31–36.

Malecki, M.T., Jhala, U.S., Antonellis, A., Fields, L., Doria, A., Orban, T., Saad, M., Warram, J.H., Montminy, M., and Krolewski, A.S. (1999). Mutations in NEUROD1 are associated with the development of type 2 diabetes mellitus. Nat. Genet. *23*, 323–328.

Nishizawa, H., Yamagata, K., Shimomura, I., Takahashi, M., Kuriyama, H., Kishida, K., Hotta, K., Nagaretani, H., Maeda, N., Matsuda, M., et al. (2002). Small heterodimer partner, an orphan nuclear receptor, augments peroxisome proliferator-activated receptor γ transactivation. J. Biol. Chem. *277*, 1586–1592.

Nishizawa, H., Matsuda, M., Yamada, Y., Kawai, K., Suzuki, E., Makishima, M., Kitamura, T., and Shimomura, I. (2004). Musclin, a novel skeletal muscle-derived secretory factor. J. Biol. Chem. *279*, 19391–19395.

Orci, L. (1974). A portrait of the pancreatic B-cell. Diabetologia *10*, 163–187.

Pontoglio, M., Sreenan, S., Roe, M., Pugh, W., Ostrega, D., Doyen, A., Pick, A.J., Baldwin, A., Velho, G., Froguel, P., et al. (1998). Defective insulin secretion in hepatocyte nuclear factor 1α-deficient mice. J. Clin. Invest. *101*, 2215–2222.

Rorsman, P., and Renström, E. (2003). Insulin granule dynamics in pancreatic beta cells. Diabetologia *46*, 1029–1045.

Stoffers, D.A., Ferrer, J., Clarke, W.L., and Habener, J.F. (1997). Early-onset type-II diabetes mellitus (MODY4) linked to IPF1. Nat. Genet. *17*, 138–139.

Takahashi, N., Kishimoto, T., Nemoto, T., Kadowaki, T., and Kasai, H. (2002). Fusion pore dynamics and insulin granule exocytosis in the pancreatic islet. Science *297*, 1349–1352.

Takahashi, N., Hatakeyama, H., Okado, H., Miwa, A., Kishimoto, T., Kojima, T., Abe, T., and Kasai, H. (2004). Sequential exocytosis of insulin granules is associated with redistribution of SNAP25. J. Cell Biol. *165*, 255–262.

Tronche, F., Ringeisen, F., Blumenfeld, M., Yaniv, M., and Pontoglio, M. (1997). Analysis of the distribution of binding sites for a tissue-specific transcription factor in the vertebrate genome. J. Mol. Biol. *266*, 231–245.

Vites, O., Rhee, J.S., Schwartz, M., Rosenmund, C., and Jahn, R. (2004). Reinvestigation of role of snapin in neurotransmitter release. J. Biol. Chem. *279*, 26251–26256.

Wada, J., and Kanwar, Y.S. (1998). Characterization of mammalian translocase of inner mitochondrial membrane (Tim44) isolated from diabetic newborn mouse kidney. Proc. Natl. Acad. Sci. USA *95*, 144–149.

Wang, H., Maechler, P., Hagenfeldt, K.A., and Wollheim, C.B. (1998). Dominant-negative suppression of HNF-1α function results in defective insulin gene transcription and impaired metabolism-secretion coupling in a pancreatic β-cell line. EMBO J. *17*, 6701–6713.

Wang, H., Antinozzi, P.A., Hagenfeldt, K.A., Maechler, P., and Wollheim, C.B. (2000). Molecular targets of a human HNF1α mutation responsible for pancreatic β-cell dysfunction. EMBO J. *19*, 4257–4264.

Winzell, M.S., and Ahren, B. (2004). The high-fat diet-fed mouse: a model for studying mechanisms and treatment of impaired glucose tolerance and type 2 diabetes. Diabetes *53* (*Suppl 3*), S215–S219.

Wollheim, C.B. (2000). Beta-cell mitochondria in the regulation of insulin secretion: a new culprit in type II diabetes. Diabetologia *43*, 265–277.

Yamagata, K., Oda, N., Kaisaki, P.J., Menzel, S., Furuta, H., Vaxillaire, M., Southam, L., Cox, R.D., Lathrop, G.M., Boriraj, V.V., et al. (1996a). Mutations in the hepatocyte nuclear factor-1α gene in maturity-onset diabetes of the young (MODY3). Nature *384*, 455–458.

Yamagata, K., Furuta, H., Oda, N., Kaisaki, P.J., Menzel, S., Cox, N.J., Fajans, S.S., Signorini, S., Stoffel, M., and Bell, G.I. (1996b). Mutations in the hepatocyte nuclear factor-4α gene in maturity-onset diabetes of the young (MODY1). Nature *384*, 458–460.

Yamagata, K., Yang, Q., Yamamoto, K., Iwahashi, H., Miyagawa, J., Okita, K., Yoshiuchi, I., Miyazaki, J., Noguchi, T., Nakajima, H., et al. (1998). Mutation P291fsinsC in the transcription factor hepatocyte nuclear factor-1α is dominant negative. Diabetes *47*, 1231–1235.

Yamagata, K., Nammo, T., Moriwaki, M., Ihara, A., Iizuka, K., Yang, Q., Satoh, T., Li, M., Uenaka, R., Okita, K., et al. (2002). Overexpression of dominant-negative mutant hepatocyte nuclear fctor-1α in pancreatic β-cells causes abnormal islet architecture with decreased expression of E-cadherin, reduced β-cell proliferation, and diabetes. Diabetes *51*, 114–123.

Yang, Q., Yamagata, K., Fukui, K., Cao, Y., Nammo, T., Iwahashi, H., Wang, H., Matsumura, I., Hanafusa, T., Bucala, R., et al. (2002). Hepatocyte nuclear factor-1α modulates pancreatic β-cell growth by regulating the expression of insulin-like growth factor-1 in INS-1 cells. Diabetes *51*, 1785–1792.

Yoshiuchi, I., Yamagata, K., Zhu, Q., Tamada, I., Takahashi, Y., Onigata, K., Takeda, J., Miyagawa, J., and Matsuzawa, Y. (2002). Identification of a gain-of-function mutation in the HNF-1β gene in a Japanese family with MODY. Diabetologia *45*, 154–155.

Zhang, H., Wada, J., Hida, K., Tsuchiyama, Y., Hiragushi, K., Shikata, K., Wang, H., Lin, S., Kanwar, Y.S., and Makino, H. (2001). Collectrin, a collecting duct-specific transmembrane glycoprotein, is a novel homolog of ACE2 and is developmentally regulated in embryonic kidneys. J. Biol. Chem. *276*, 17132–17139.